

Penguin Locomotion: Robotic Aquaflaying Wings

Jose Luis Santiago

Abstract—A study and decomposition of the way penguins fly through water using their wings as propulsive mechanisms. Modeling of the locomotion is done in MATLAB. The wing is a penguin’s main proponent of thrust. Previous studies have researched the propulsive properties of penguin wings by fabricating hydrofoil models that are similar in shape to penguin wings, or fabricating 3D printed models of wings derived from scanned live penguin wings. This paper expands on their research by simulating the dynamic properties of swimming for different-sized penguin wings, such as those of the Emperor and King penguins.

Index Terms—Three Degrees of Freedom, Angle of Attack, Drag, Drag Coefficient, Lift, Lift Coefficient, Pitch, Feathering, Flapping, Bio-mimicry



Fig. 1. Gentoo Penguins at the Errera Channel–Danco Island, Antarctica, shot by James Holmes. <https://macaulaylibrary.org/asset/98575351>

I. INTRODUCTION

PENGUINS are flightless birds that have re-purposed their wings to act as hydrofoils that can propel them through water, giving them the ability to swim. Although penguins use their wings to propel them through water, their wing stroke has been described as similar to that of flying birds [3]. Penguin wings are reduced in length and area when compared to wings of flying birds, furthermore the supracoracoideus (muscle responsible for wing elevation in birds) is quite large in penguins [3]. These qualities of the penguin wing anatomy point to how they have adapted to swimming. The large supracoracoideus shows an increase in effort required of penguins to elevate their wings underwater. Extensive research of robotic swimming

locomotion of fish caudal fins has been done [6], but penguins, which rely on their wings for propulsion, have not been studied as closely. This leads researchers to explore the possibility that a wide range of thrust and torque can be generated by controlling the wings of a penguin.

Penguin bio-mimetic robot implementation research is scarce. I was only able to find two research papers that detailed the fabrication of an actual penguin wing robot with three degrees of freedom [1][2]. The research done in the article “Robotic Penguin-like Propulsor with Novel Spherical Joint” details a robotic wing implementation that uses a novel spherical joint along with a hydrofoil to imitate the propulsive qualities of a penguin wing [2]. The research paper detailed the fabrication of their wing, but it did not detail the mathematical models of the wing motion. Because of this the paper was not useful for my research, but I thought it was worth mentioning since they did create a robotic penguin wing.

The second paper, “Biomimetic Realization of a Robotic Penguin Wing: Design and Thrust Characteristics”, detailed more about the kinematic study behind the penguin swimming locomotion as well as the mathematical models that describe their motion.

A. Biomimetic Realization of a Robotic Penguin Wing: Design and Thrust Characteristics

This research paper has been the most useful to me in my study as it has given me a base mathematical model to work with. This paper details a kinematic study of a Gentoo penguin prior to the fabrication of a robotic wing. The researchers in the article use twelve waterproof cameras to examine a Gentoo penguin’s swim pattern. The cameras were mounted in a water tank 14m in length, 4m in width, and 4m in depth. Three markers on each wing were used for the motion analysis of the wings.

One main takeaway from the kinematic study was the decomposition of the wing motion into three rotational degrees of freedom: flapping, feathering, and pitch. These components all contribute to the Angle of Attack (AoA), which is a crucial parameter in fluid dynamics. The AoA is defined as the angle between the inflow vector and the wing plane. It directly influences the thrust performance of the penguin wing.

Another big takeaway from the study was the pattern the flapping motion the Gentoo penguin wing followed. Based on their measurements it was found that flapping and feathering motion are almost sinusoidal with an average amplitude of 40° and 20°, respectively. This means they could approximate both flapping and feathering to sinusoids to simplify their

mathematical models. In their preliminary analysis they use a reference point A (located at 75% the length of the wing) to do their modeling.

To model the change in the angles along the flapping, feathering, and pitch rotational axes, the researchers used sinusoids as follows:

$$\begin{aligned}\theta_{flap} &= A_{flap} \sin(2\pi ft) \\ \theta_{feather} &= A_{feather} \sin(2\pi ft - \frac{\pi}{2}) \\ \theta_{pitch} &= A_{pitch}\end{aligned}\quad (1)$$

Flapping and feathering rotational axes are modeled with sinusoids, where the phase of the feathering angle is $\frac{\pi}{2}$ behind the phase of the flapping angle. A_{flap} and $A_{feather}$ are the amplitudes of flapping and feathering motions, respectively. The frequency of the θ_{flap} and $\theta_{feather}$ sinusoids are equal and are represented by the f variable in eq. (1). A_{pitch} is a constant amplitude since it was not considered in this portion of their study. The flapping, feathering, and pitch rotational axes can be seen in the following figure:

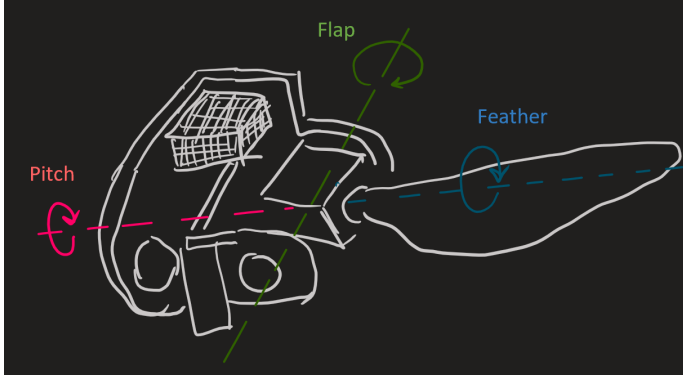


Fig. 2. Visualization of the flapping, feathering, and pitch rotational axes. Notice that feathering and pitch are on the same axis, but feathering occurs about the wing, while pitch occurs about the whole theoretical penguin body.

To model the position of the point A with regards to the changing flapping and feathering angles, they used a rotational transformation matrix:

$$R_W^B = R(\theta_{pitch})R(\theta_{flap})R(\theta_{feather}) \quad (2)$$

where $R(\theta_{pitch})$, $R(\theta_{flap})$, and $R(\theta_{feather})$ are rotational matrices that result from the pitch, flap, and feather rotations respectively:

$$R(\theta_{pitch}) = \begin{bmatrix} \cos(\theta_{pitch}) & -\sin(\theta_{pitch}) & 0 \\ \sin(\theta_{pitch}) & \cos(\theta_{pitch}) & 0 \\ 0 & 0 & 1 \end{bmatrix}$$

$$R(\theta_{flap}) = \begin{bmatrix} 1 & 0 & 0 \\ 0 & \cos(\theta_{flap}) & -\sin(\theta_{flap}) \\ 0 & \sin(\theta_{flap}) & \cos(\theta_{flap}) \end{bmatrix} \quad (3)$$

$$R(\theta_{feather}) = \begin{bmatrix} \cos(\theta_{feather}) & -\sin(\theta_{feather}) & 0 \\ \sin(\theta_{feather}) & \cos(\theta_{feather}) & 0 \\ 0 & 0 & 1 \end{bmatrix}$$

The reference position on the wing, A, was modeled with a vector representing the x, y and z axes respectively when the flapping angle is 0° as follows:

$$r_W = \begin{bmatrix} 0 \\ 0 \\ r_A \end{bmatrix} \quad (4)$$

where r_A is the distance from the origin of the wing to point A, located at 75% of the wing length.

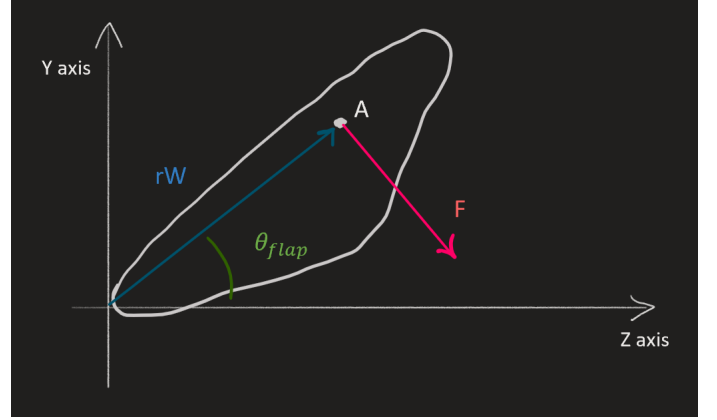


Fig. 3. Free body diagram of the wing as it moves through the ZY plane. It also depicts what the wing would look like in the ZY plane

After completion of the kinematic study, the researchers moved on to fabrication of the robotic penguin wing. The design they chose used three servo motors to actuate the robot wing. The flipper was made from a 3D scan of the live Gentoo penguin used in the kinematic study mentioned previously. The scanned wing model was scaled down to 0.4 times the original size. The wing cross sections were close to symmetric so they were modified to be fully symmetric for simplicity. The model was 3D printed as 8.7 grams of tough PLA with a surface area of 2256mm^2 and wing length of 101mm .

After successfully creating a robotic penguin flipper, they did a hydrodynamic study of the wing at different angles of attack, dictated by the feathering angle. The feathering angle and AoA have an inversely proportional relationship. The larger the feathering angle, the smaller the AoA.

From this study they found that the maximum net thrust is achieved with the combination of flapping amplitude of 50° and a feathering amplitude of 25° . The AoA for the maximal thrust was recorded as 33° . With this AoA, the optimal Lift-to-Drag ratio was recorded as 1.49, with the following Lift and Drag coefficients:

$$\begin{aligned}C_L &= 1.1 \\ C_D &= 0.73\end{aligned}\quad (5)$$

B. Kinematics of Swimming Penguins at the Detroit Zoo

Another useful paper for understanding penguin swimming locomotion was “Kinematics of Swimming Penguins at the Detroit Zoo,” by B.D. Clark and W. Bemis [3]. In this paper, the researchers studied penguins at the Detroit Zoo Penguinarium. They used different kinds of film recordings

to study the penguins' movement. They studied the wingbeat cycle of penguins in detail. Some important properties of the wingbeat cycle that were noted were: wingbeat frequency, wingbeat amplitude, stride length, gliding phases, directional control, and drag coefficient.

II. METHODS

The methods I employed to study penguin wing propelled swimming involve the use of MATLAB, along with the equations I mentioned earlier (eq. (1-5)) from my review of "Biomimetic Realization of a Robotic Penguin Wing: Design and Thrust Characteristics." A difference in my approach from theirs is that I did not include the pitch rotational axis. I did this to simplify my model. For this reason I decided it would be best to start with flapping first. I did not want to complicate things with more dimensions than I could handle at the beginning of my research. For simplification I also assume that the penguin is only swimming in a forward motion with neutral buoyant forces.

The first thing I did was model the change in the θ_{flap} and $\theta_{feather}$ angles of the penguin wing. To model these I plotted eq. (1) in MATLAB. From there I could derive the motion via the change in position of the reference point A (located at 75% of the length of the penguin wing). To see the change in position of reference point A with the changing θ_{flap} , I multiplied the rotational transformation matrix equation (eq. 2) by the vector of reference point A (eq. 4):

$$A_{ZY} = R_W^B r_W \quad (6)$$

where A_{ZY} denotes the position of the reference point A in the ZY plane. This equation gave me an idea of what the penguin wing would look like in the ZY axis as it flaps up and down.

After this I calculated the derivative of the position A_{ZY} (eq. 6) in MATLAB to describe the velocity of the wing at reference point A as it flaps in the ZY plane:

$$v_A = \frac{d}{dt} A_{ZY} \quad (7)$$

where v_A denotes the velocity of reference point A.

Following this I took the first derivative of the velocity of reference point A (eq. 7) (or the second derivative of the position of reference point A (eq. 6)) so I could get the acceleration of reference point A on the wing:

$$a_A = \frac{d^2}{dt^2} A_{ZY} = \frac{d}{dt} v_A \quad (8)$$

where a_A denotes the acceleration of reference point A.

With these derivations I could calculate the force of the wing as it flaps up and down. Since the mass (8.7g) and length (101mm) of the Gentoo penguin wing were measured and known from the research paper "Biomimetic Realization of a Robotic Penguin Wing," I was able to depict the force in the Y and Z axes. As long as I have the length of a penguin wing, as well as its mass I will be able to model all these different aspects of the wing motion for different sized penguin wings.

Although the force of the wing (with no external forces considered) would look identical to the acceleration multiplied to a different magnitude ($F = ma_A$), I thought it would be

useful to know. An aspect of the forces at play for swimming locomotion that is of more importance are Lift and Drag. Since we adopted Lift and Drag coefficients from "Biomimetic Realization of a Robotic Penguin Wing," we are able to find the Lift and Drag of a Gentoo penguin wing scaled to different sizes. The Lift and Drag equations used for this derivation are as follows:

$$\begin{aligned} L &= \frac{1}{2} C_L \rho v_A^2 S \\ D &= \frac{1}{2} C_D \rho v_A^2 S \end{aligned} \quad (9)$$

where ρ is the fluid density of the water the penguin wing is flapping in, v_A is the velocity of reference point A on the wing, and S is the surface area of the penguin wing. C_L and C_D are the Lift and Drag coefficients respectively (eq. 5). I used the Lift and Drag equations and scaled the penguin wing model up and down (by increments of 0.2 times the original size, from 0.2 to 2.0 times the original wing model size) to observe the different Lift and Drag of different sized Gentoo penguin wings.

III. RESULTS

An analysis of the results from the study detail a clearer picture of the forces at play in the penguin wing. Fig. 4 depicts the change in θ_{flap} and $\theta_{feather}$ in one second. I used eq. (1) to model these sine waves. I chose the amplitude of the flapping angle as 50° and the amplitude of the feathering angle as 25° , since those values were recorded to provide the maximum thrust [1]. In addition, the frequency of both is equal to $1.8 \frac{\text{cycles}}{\text{second}}$. The motion of the change in angle can be seen below and follows what is expected from a sinusoid.

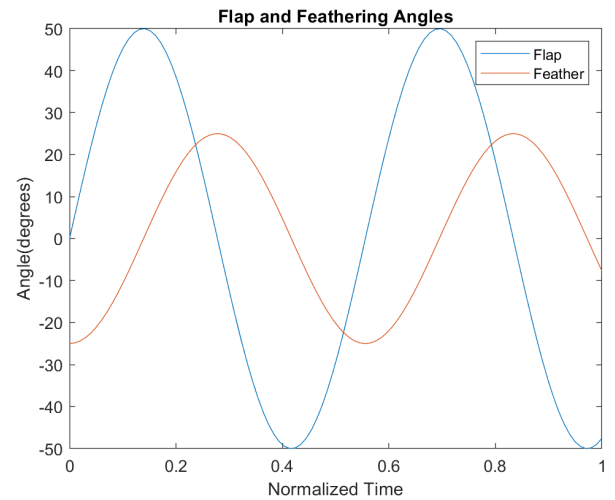


Fig. 4. Sinusoidal motion of the change in flapping and feathering angles of our theoretical penguin wing

Following this derivation I moved on to explore the position of the reference point A as the flapping and feathering angles change, as shown above in Fig. 4. To do this I used the position equation (A_{ZY}) derived in the Methods section (eq. 6). After plotting the values I received from inputting the different sine values, I was able to come up with a depiction of how the

wing was rotating on the ZY plane. Fig. 5 shows the motion of the wing through the plane, while Fig. 3 shows a visual representation of what the wing would look like if you took a snapshot of it at one frame of its motion. The gradual change

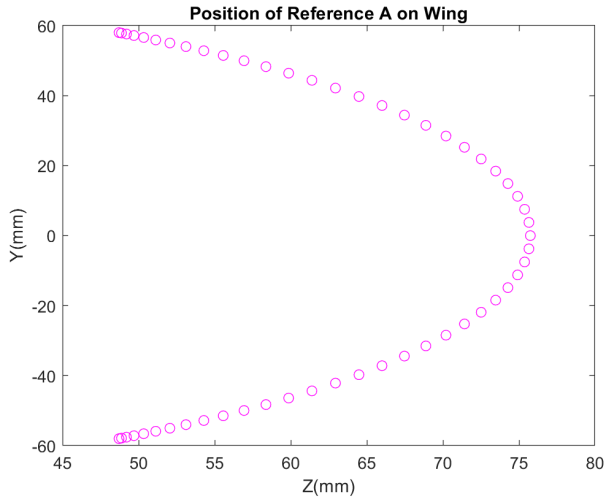


Fig. 5. Position of reference point A (located at 0.75% of the wing length) in the Z and Y axes derived from the position of point A from Fig. 5

in position of the reference point A depicted in Fig. 5 is what should be expected if the wing from Fig. 3 was flapping.

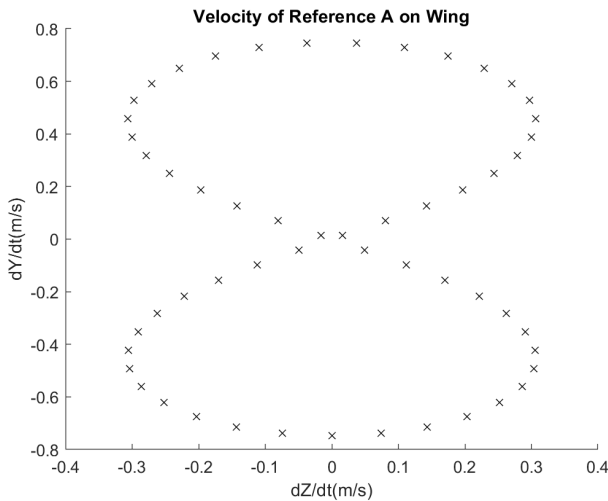


Fig. 6. Velocity of reference point A (located at 0.75% of the wing length) in the Z and Y axes derived from the position of point A from Fig. 5

Fig. 6 depicts the velocity of the wing as it flaps by using eq. (7). This figure also looks as expected from the wing motion. Since the wing is going back and forth in a symmetric manner, it makes sense that the velocity would be symmetric as well. The way it is symmetric about zero shows that the motion stops and restarts when the maximum amplitude of the flapping angle ($\theta_{flap} = 50^\circ$) is reached in the positive and negative direction. We can see here how the wing is changing direction where the points converge at $0 \frac{mm}{s}$. We can tell it is changing direction because the velocity changes sign as it crosses the zero. We can see the minimum and maximum

velocities of the wing in the Z axis are $-0.3 \frac{m}{s}$ and $0.3 \frac{m}{s}$, respectively. We can also see that the minimum and maximum velocities in the Y axis are $-0.8 \frac{mm}{s}$ and $0.8 \frac{mm}{s}$, respectively.

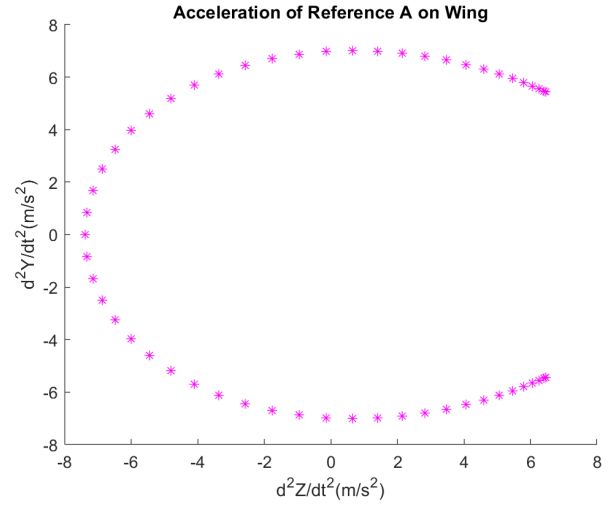


Fig. 7. Acceleration of reference point A (located at 0.75% of the wing length) in the Z and Y axes derived from the velocity of point A from Fig. 6

Fig. 7 depicts the acceleration of reference point A on the wing using eq. (8). Looking at this figure we can see how the wing speeds up and slows down as the wing flaps back and forth from positive to negative amplitudes ($-50^\circ, +50^\circ$). This figure shows how the wing speed is effected in the Z and Y axes.

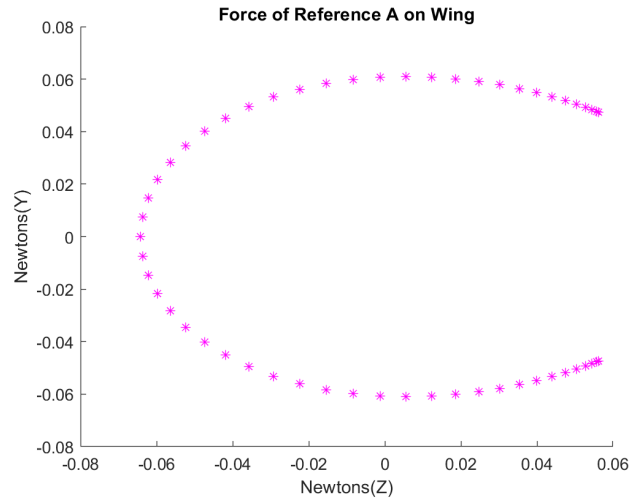


Fig. 8. Force of reference point A (located at 0.75% of the wing length) in the Z and Y axes derived from the acceleration of point A from Fig. 7

Fig. 8 depicts the force of the wing as it travels through the dictated flapping angle range ($-50^\circ, +50^\circ$). This figure looks identical to the previous one, but with a different magnitude since it was multiplied by the mass of the wing and converted into Newtons.

Now that the kinematics of the penguin wing have been described, we can begin to analyze the hydrodynamic aspects of the flapping wing. As previously mentioned, we are using a

flapping amplitude of 50° with a feathering amplitude of 25° to achieve maximum thrust of the wing. Assuming an AoA of 33° we can use the coefficients of Lift and Drag found from our research (eq. 5) in combination with the given penguin wing dimensions [1], and my velocity derivation (eq. 7), to find the Lift and Drag (eq. 9).

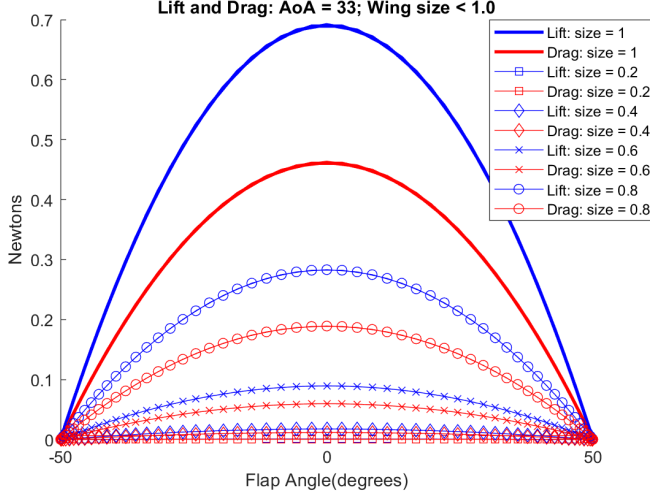


Fig. 9. Lift and Drag of a wing scaled to sizes less than the original reference scale size (denoted as size = 1). Lift is shown in blue, while Drag is shown in red.

Fig. 9 shows the different Lift and Drag values for the wing as it flaps from the given θ_{flap} amplitude range (-50° , $+50^\circ$). There are also Lift and Drag plots for the wing in different scales less than the original size (size = 1). The decrements are in 0.2 of the original wing model size. From this plot we can see that the Lift and Drag decrease as the size of the penguin wing is scaled down.

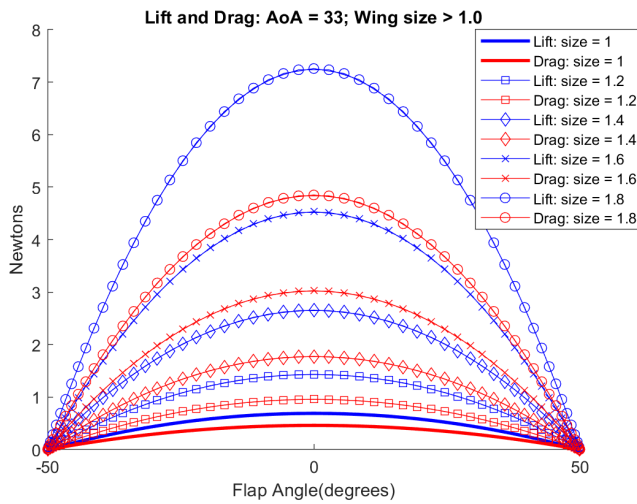


Fig. 10. Lift and Drag of a wing scaled to sizes greater than the original reference scale size (denoted as size = 1). Lift is shown in blue, while Drag is shown in red.

Fig. 10 shows the different Lift and Drag values for the wing as it flaps from the given θ_{flap} amplitude range (-50° , $+50^\circ$). There are also Lift and Drag plots for the wing in different

scales greater than the original size (size = 1). The increments are in 0.2 of the original wing model size. From this plot we can see that the Lift and Drag increase as the size of the penguin wing is scaled up.

The results from this hydrodynamic study show a positive correlation between the size of the penguin wing and the Lift and Drag forces generated. This is not accurate with the true properties of the biological penguin wing.

Due to the square-cube law, we know that if an object increases in scale by x amount, the surface area increases by x^2 , and the mass increases by x^3 . This means that as mass increases to the third degree, area increases to the second. This implies that the cross-sectional area of muscle (which grows to the second degree) is not able to grow with the proportions necessary to move the mass of the wing (which grows to the third degree).

Despite this, since we are working in water the effects of buoyancy mean the implications of increase in mass are reduced. This means the wing can grow more in water than it would be able to grow in open air because of the force of buoyancy. This is why large animals (for example the blue whale, the largest-known animal to exist on Earth) are able to survive in the ocean.

Even with the buoyant force, at some point the load of the mass will be too great for the wing to be able to propel the penguin with optimal thrust to prove useful and agile as found in nature. Although it was not found in this paper, there is a target range for the wing size where the thrust will be optimal and prove the most effective for swimming underwater.

IV. CONCLUSION

This paper details the kinematics of the penguin wing flapping. First I explore the kinematics of the penguin wing as it flaps in open air with no external forces. I specifically depict the position, velocity, acceleration, and force of the penguin wing. Then I test different hydrodynamic properties (Lift and Drag) that different-sized penguin wings have as they flap and exert force in water.

We can conclude from this study that we can achieve a larger Lift with larger penguin wings, but we would need motors strong enough to actuate the wing. At some point the wing will succumb to the mass and be unable to move in an optimal way to prove useful in locomotion.

Further research needs to be done in order to identify the optimal penguin wing model for swimming locomotion. The critical point for the size of a wing which provides the best Lift and Drag without sacrificing agility is yet to be found. This paper introduces a structure for further research on the topic.

APPENDIX A

TABLE 1

Nomenclature	
θ_{flap}	The angle in degrees of the wing in the flapping rotational axis
$\theta_{feather}$	The angle in degrees of the wing in the feather rotational axis
θ_{pitch}	The angle in degrees of the wing in the pitch rotational axis
A_{flap}	The amplitude of the sinusoid describing the change in angle of the flap rotational axis
$A_{feather}$	The amplitude of the sinusoid describing the change in angle of feather rotational axis
A_{pitch}	The constant value describing the angle of the angle in the pitch rotational axis
f	The frequency of the sinusoid describing the change in angle of the flap and feather axes
R_W^B	The rotational transformation matrix which describes the change in position of the wing, depending on the value of θ_{flap} , $\theta_{feather}$, and θ_{pitch}
$R(\theta_{pitch})$	The rotation matrix describing the change in position of the wing depending on the value of θ_{pitch}
$R(\theta_{flap})$	The rotation matrix describing the change in position of the wing depending on the value of θ_{flap}
$R(\theta_{feather})$	The rotation matrix describing the change in position of the wing depending on the value of $\theta_{feather}$
A	The reference point A of the wing. It is located at 75% of the wing length
r_w	The position vector describing the position of reference point A on the wing
r_A	The distance from the origin of the wing reference frame to reference point A
A_{YZ}	The position of reference point A in the YZ plane
v_A	The velocity of reference point A in the YZ plane
a_A	The acceleration of reference point A in the YZ plane
D	The drag force of the penguin wing
L	The lift force of the penguin wing
C_D	The coefficient of drag of the penguin wing
C_L	The coefficient of lift of the penguin wing
α	The angle of attack (AoA) of the penguin wing. The angle between the inflow vector and the wing plane.
ρ	The fluid density of the water the penguin is swimming in
S	The surface area of the penguin wing

REFERENCES

- [1] Y. Shen, N. Harada, S. Katagiri and H. Tanaka, *Biomimetic Realization of a Robotic Penguin Wing: Design and Thrust Characteristics*, in IEEE/ASME Transactions on Mechatronics. 2020. doi: 10.1109/TMECH.2020.3038224.
- [2] B. Sudki, M. Lauria, F. Noca. *Robotic Penguin-like Propulsor with Novel Spherical Joint*. 2013.
- [3] B.D. Clark, W. Bemis. *Kinematics of swimming of penguins at the Detroit Zoo*. Journal of Zoology, 188: 411-428. 1979. <https://doi.org/10.1111/j.1469-7998.1979.tb03424.x>
- [4] C. A. Hui, *Penguin Swimming. I. Hydrodynamics*, Physiological Zoology. [Online]. Available: <https://www.journals.uchicago.edu/doi/abs/10.1086/physzool.61.4.30161251>. [Accessed: 15-Feb-2021].
- [5] T. A. van Walsum, *Research Report 1 : Penguin flipper hydrodynamics*, Student Theses Faculty of Science and Engineering, 01-Jan-1970. [Online]. Available: <https://fse.studenttheses.ub.rug.nl/12053/>. [Accessed: 15-Feb-2021].
- [6] A. H. Techet, *Propulsive performance of biologically inspired flapping foils at high Reynolds numbers*, Journal of Experimental Biology, vol. 211, no. 2, pp. 274–279, Jan. 2008, doi: 10.1242/jeb.012849.
- [7] J. R. Lovvorn, *Upstroke Thrust, Drag Effects, and Stroke-glide Cycles in Wing-propelled Swimming by Birds*, American Zoologist, vol. 41, no. 2, pp. 154–165, 2001.
- [8] K. Sato, K. Shiomi, Y. Watanabe, Y. Watanuki, A. Takahashi, P.J. Ponganis. *Scaling of swim speed and stroke frequency in geometrically similar penguins: they swim optimally to minimize cost of transport*. Proc. R. Soc. B.277707–714. 2010.
- [9] K. Sato, Y. Watanuki, A. Takahashi, P.J. Miller, H. Tanaka, R. Kawabe, P.J. Ponganis, Y. Handrich, T. Akamatsu, Y. Watanabe, Yo Mitani, D.P. Costa, C.A. Bost, K. Aoki, M. Amano, P. Trathan, A. Shapiro, Y. Naito. *Stroke frequency, but not swimming speed, is related to body size in free-ranging seabirds, pinnipeds and cetaceans*. Proc. R. B.274471–477. 2006. <http://doi.org/10.1098/rspb.2006.0005>